Neurospine 2025;22(3):696-712.
https://doi.org/10.14245/ns.2551050.525

Neurospine
pISSN 2586-6583 eISSN 2586-6591

Review Article

Corresponding Author
Misao Nishikawa
https://orcid.org/0000-0002-0808-390X

Department of Neurosurgery, Moriguchi Ikuno Memorial Hospital, 6-17-33 Satanakamachi, Osaka 570-0002, Japan
Email: misaonishikawa88@gmail.com

Received: July 12, 2025
Revised: September 3, 2025
Accepted: September 9, 2025

Chiari Malformation and Hindbrain Descent: Characterization and New Classification Based on Mechanism and Pathogenesis, and Surgical Management

Misao Nishikawa[1,2], Paolo A. Bolognese[3], Masaki Yoshimura[4], Kentarou Naito[2], Noritsugu Kunihiro[5], Hiromichi Ikuno[6], Mitsuhiro Hara[7], Hiroaki Sakamoto[5], Kenji Ohata[8], Takeo Goto[2]

[1]Department of Neurosurgery, Moriguchi Ikuno Memorial Hospital, Moriguchi, Japan
[2]Department of Neurosurgery, Osaka Metropolitan University Hospital, Osaka, Japan
[3]Chiari EDS Center, Mount Sainai South Nassou University Hospital, Oceanside, NY, USA
[4]Department Neurosurgery, Tokusyukai Yao General Hospital, Yao, Japan
[5]Department of Pediatric Neurosurgery, Osaka City General Hospital, Osaka, Japan
[6]Department of Neuroradiology, Moriguchi Ikuno Memorial Hospital, Osaka, Japan
[7]Department of Neurology, Moriguchi Ikuno Memorial Hospital, Osaka, Japan
[8]Department of Neurosurgery, Naniwa Ikuno Hospital, Osaka, Japan

H. Chiari described 4 types of abnormal development of the posterior fossa, which were subsequently classified as Chiari malformation types I, II, III, and IV. Many issues in neurosurgery concerning classification and surgical management are without evolving concepts. This review aims to clarify the mechanisms and pathogenesis underlying hindbrain (the brain stem and cerebellum) descent, classify them accordingly, and discuss appropriate surgical management. We propose a classification of 4 independent pathogenic mechanisms: (1) constriction in the posterior cranial fossa (PCF) due to underdevelopment of the occipital bone; (2) enlargement of hindbrain; and (3) traction caused by tethering lesions. We examine the pathogenesis of hindbrain descent from embryological perspectives and neuroradiological findings, with a particular focus on lesser-known mechanisms. Additionally, another fourth mechanism is proposed: (4) instability at the craniocervical junction. We suggest a novel classification for Chiari malformation type I based on the underlying pathogenesis, guided by morphometric (occipital bone size) and volumetric (PCF volume) analyses. Furthermore, it delves deeper into their pathogenesis by drawing on insights from developmental biology, genetic studies, and experimental research. Surgical management is tailored to the underlying mechanism, and we proposed the algorithm for decision of surgical intervention. For crowding of the PCF due to underdevelopment of the occipital bone, posterior fossa decompression is the appropriate surgical intervention. For craniocervical instability, occipitocervical fixation is recommended. We also review the recent literature on surgical outcomes associated with each treatment approach. Finally, we highlight current genetic research related to the pathogenesis of hindbrain descent.

Keywords: Chiari malformation, Classification, Genetic research, Pathogenesis, Tonsillar herniation, Surgical management

This is an Open Access article distributed under the terms of the Creative Commons Attribution Non-Commercial License (https://creativecommons.org/licenses/by-nc/4.0/) which permits unrestricted non-commercial use, distribution, and reproduction in any medium, provided the original work is properly cited.

Copyright © 2025 by the Korean Spinal Neurosurgery Society

BACKGROUND AND INTRODUCTION

In articles published in 1881 and 1886, H. Chiari described 4 types of abnormal development of the posterior fossa, which have subsequently been classified as Chiari malformation types I, II, III, and IV.[1,2] Chiari malformation type II (CM-II) is characterized by a suboccipital meningoencephalocele, while type IV involves cerebellar agenesis. However, both anomalies are extremely rare and are not discussed further in this review. The designation "CM-II" should be reserved for patients with concomitant spina bifida cystica. Arnold's name was also added to the term for this complex abnormality of the posterior fossa structures and the content of the upper cervical spinal canal, i.e., "Arnold-Chiari malformation;" however, this condition is now generally referred to simply as "Chiari malformation."[3]

Chiari's original articles focused on hydrocephalus, and it remains unclear whether the hindbrain herniation described was the cause or result of hydrocephalus.[1,2] What has come to be known as Chiari malformation type I (CM-I) is characterized by herniation of the cerebellar tonsils through the foramen magnum. There appears to be no logical reason to associate Arnold's name with this particular malformation. Moreover, many cases of CM-I are not only acquired but also potentially reversible; thus, the term "hindbrain descent" might better describe this condition. Nevertheless, the designation CM-I has become a well-recognized term, clearly understood in diagnostic and surgical treatment contexts.[4,5]

Since the introduction of magnetic resonance imaging (MRI) as a diagnostic modality in the 1980s, it has rapidly replaced myelography and become the most widely used neuroimaging technique. Some studies have revealed that even asymptomatic individuals may present with a mild degree of tonsillar herniation (TH). As a general rule, neuroradiologists suggest a diagnosis of CM-I when the tip of one or both tonsils extends more than 3–5 mm below the basion-opisthion line (McRae line).[6,7] In healthy adults, the cerebellar tonsils are usually located above the foramen magnum; however, textbooks continue to define TH into the spinal canal as > 3–5 mm beyond McRae line.[8]

According to the degree of TH, several subtypes have been introduced, including CM-0, CM-0.5, and CM-1.5. Iskandar et al. described a group of pediatric patients with syringomyelia, but without TH, who improved following posterior fossa decompression and C1 laminectomy, suggesting a Chiari-like pathophysiology.[9-13] They hypothesized that a small posterior fossa and a tight cisterna magna could explain this condition, leading to the introduction of CM-0 and CM-0.5.[9-13] Tubbs et al. later coined the term CM-1.5 to define a phenotype intermediate between CM-I and CM-II, but not associated with neural tube defects.[14] The hallmark of CM-1.5 is the presence of TH along with caudal descent of the brainstem, with the obex located below McRae line.[14] Despite presenting with symptoms similar to those of CM-I, these variants may require different surgical strategies, making accurate classification critical.[9-15]

What follows is a discussion of the pathogenesis, classification, and surgical management of CM-I. Few topics in neurosurgery remain as debated as the classification and treatment of this condition. This review focuses on: (1) clarifying the mechanisms behind hindbrain descent; (2) proposing a new classification of CM-I based on morphometric and volumetric studies; (3) suggesting surgical approaches tailored to the underlying pathogenesis; and (4) reviewing recent genetic research related to the mechanisms of hindbrain descent.

HYPOTHESES REGARDING THE CAUSES AND MECHANISMS OF CM-I INVOLVING THE HINDBRAIN DESCENT

If we consider the mechanism of hindbrain descent in a simplified manner, the following hypotheses can be proposed:

Mechanism #1: Constriction of the posterior cranial fossa (PCF). The PCF, which serves as a container for the hindbrain, is too small, causing the normally developed hindbrain to herniate into the spinal canal.

Mechanism #2: Overgrowth of the hindbrain. Although the PCF continues to grow and develop normally, the hindbrain is too large, leading to its herniation into the spinal canal.

Mechanism #3: Traction due tethering. The hindbrain is pulled downward from below (caudally), resulting their herniation into the spinal canal.

Mechanism #4: "Cranial settling" and "posterior gliding" of occipital condyle due to instability and hypermobility at the occipito-atlas-axis joints (craniocervical junction [CCJ]).

This article reviews these 4 hypotheses about mechanism of the hindbrain descent, including past reports and the author's own findings. Furthermore, it delves deeper into their pathogenesis by drawing on insights from developmental biology, genetic studies, and experimental research. At first, we tried to clarify the mechanism of the hindbrain descent based on the volumetric and morphometric analyses of PCF and CCJ, and discussed the pathogenesis of the hindbrain descent induced from the phenotype clarification.

MATERIALS: VOLUMETRIC AND MORPHOMETRIC ANALYSES OF PCF AND CCJ

1. Normal Controls and Inclusion Criteria

This study recruited 150 normal volunteers (controls) with no neurological symptoms or abnormalities in the neural axis (aged 4–49 years; mean, 18.7 years; 64 males and 86 females). In addition, 449 patients with CM-I (cerebellar tonsil herniation ≥ 5 mm from the McRae line, i.e., between the basion and opisthion) presence of brainstem symptoms and/or myelopathy were included (aged 4–49 years; mean, 18.1 years; 204 males and 245 females) and 37 patients with CM-borderline (cerebellar tonsil herniation < 5 mm from the McRae line, but presence of brainstem symptoms and/or myelopathy) (aged 5–45 years; mean, 18.4 years; 15 males and 22 females). The distribution and mean of age and sex were not significantly different between normal controls and CM-I group. These patients were diagnosed and treated between April 2006 and March 2020. All of normal controls and patients were selected from Asian (Asian American, Asian European, Chinese, Korean, and Japanese), considering ethnic variation. Both normal controls and patients were managed in The Chiari Institute North Shore University Hospital, New York USA, Osaka City University Hospital, Osaka City General Hospital and Moriguchi Ikuno Memorial Hospital.

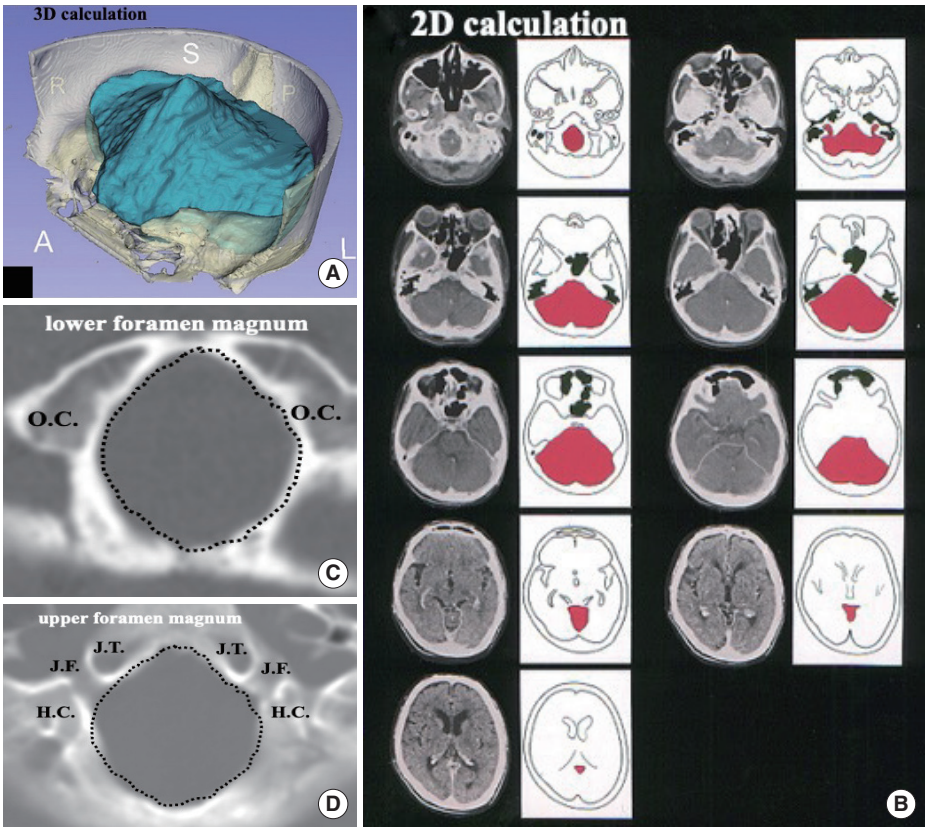

Fig. 1. Volumetric calculation of the posterior cranial fossa (PCF). (A) Three-dimension computed tomography (3D-CT) reconstructed image of the PCF using Osirix software. (B) Two-dimensional (2D)-CT images of the PCF. Red areas indicate the volume of PCF. (C) 2D-CT image demonstrating the area of the inferior outlet of the foramen magnum at the level of the basion and opisthion. (D) 2D-CT image demonstrating the area of the superior outlet of the foramen magnum at the level of the jugular tubercle. The PCF was defined as the almost circular space bounded by the tentorium cerebelli, occipital bone, clivus, petrous bone, and petrous ridges. The ridges of the petrous bones form the anterolateral border of the cavity, and their connection to the posterior clinoids (posterior petroclinoid ligament) forms the anterior border. The caudal end of PCF was defined as the foramen magnum, including the McRae line. McRae line was defined as the line between the basion and opisthion. The volume of brain in PCF was calculated as the neural content of the PCF, including the cerebellum, mesencephalon, pons, and medulla (blue areas in A, and red areas in B). A, anterior; P, posterior; L, left; R, right; S, superior; H.C., hypoglossal nerve canal; J.F., jugular foramen; J.T., jugular tubercle; O.C., occipital condyle.

https://doi.org/10.14245/ns.2551050.525

2. Exclusion Criteria

The cases who had myelopathy and/or radiculopathy due to disc hernia, spondylotic change and ossification of the longitudinal ligament were excluded. The cases older than 50 years old was excluded, because they were affected the factors of ageing of the brain and degeneration of the bony structures etc. The infant and toddler younger 4 years old were excluded, because in this age the development and growth is very rapid and there is risk by radiation.

METHODS: VOLUMETRIC AND MORPHOMETRIC ANALYSES OF PCF AND CCJ

1. Volumetric and Morphometric Analyses of PCF and Hindbrain (Figs. 1 and 2)

We used 2D- or 3-dimensional (3D)-CT reconstructed images with Osirix software (free access) to calculate the volume of PCF (PCFV) (Fig. 1A and B), volume of surrounding area of foramen magnum (VAFM, i.e., total volume between the inferior and superior outlets of the foramen magnum) (Fig. 1C and D).[16-18] PCFV was divided into the volume of the area of above Twining line and below Twining line. The volume of the brain in the posterior cranial fossa (PBFV) was calculated on MRI axial and sagittal images, excluding the 4th ventricle (4VH), herniated cerebellar tonsils, and medulla oblongata.

On 2D-CT coronal images at the occipital condyle and midline sagittal plane, the axial length of the basiocciput (clivus), exocciput (condyle), and supraocciput as enchondral parts of the occipital bone (occipital bone size) were measured (Fig. 2A and B). Using MRI midline image, the axial length of the brain stem, medullary height (MH), and the position of 4VH were measured (Fig. 2C).[6-18] CM-I was categorized on the basis of multiple analyses of the results. The radiographic analysis was performed using Osirix software.

2. Morphometric Measurements and Evaluation of CCJ Instability (Fig. 3)

CCJ instability was diagnosed using a morphometric study and craniocervical traction test, which were described by the authors and Goel et al. in past reports and a textbook.[16,18-23] For the craniocervical traction test, a tong was attached to the skull

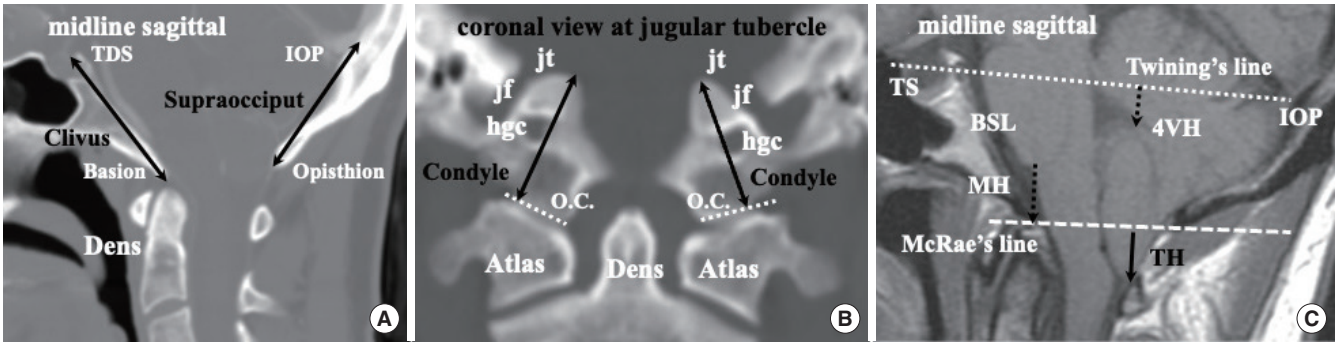

Fig. 2. Morphometric measurements of enchondral parts of occipital bone. (A) Two-dimension computed tomography (2D-CT) midline sagittal image demonstrating morphometric measurements of the basiocciput (clivus) (left black double arrow) and supraocciput (right black double arrow). (B) 2D-CT coronal image at the hypoglossal nerve canal (hgc) and jugular tubercle (jt). Demonstrating morphometric measurements of the exoocciput (condyle) (double lack arrows). jf, jugular foramen; O.C., articular process of occipital condyle (white dotted lines). (C) Magnetic resonance imaging midline sagittal image demonstrating morphometric measurements of the axial length of the brain stem (BSL) (large black dotted line), medullary height (MH) (black small dotted line), and the position of the 4th ventricle (4VH) (black small dotted line). IOP, the internal occipital protuberance; TDS, top of tuberculum sellae (TS); Twining line, the line between the TS and internal occipital protuberance (IOP); McRae line, the line between the basion and opisthion; TH, tonsilar herniation (black arrow). Measurements included the axial length of the clivus (basiocciput and basisphenoid) from the top of the dorsum sellae to the basion; the axial length of the supraocciput from the center of the IOP to the opisthion; and the axial length of the occipital condyle (exocciput) from the top of the jugular tubercle to the bottom of the occipital condyle and the supraocciput (distance between the opisthion and the center of the IOP): these 3 measurements were unified as occipital bone size. The axial BSL was defined between the midbrain-pons junction and medullo-cervical junction. MH was defined the vertical distance between the ponto-medullary junction and McRae line. The position of the 4VH was defined as the vertical distance between the fastigium (transverse summit of the roof of fourth ventricle) of the 4th ventricle and Twining line. TH means the length of herniation of the cerebellar tonsils.

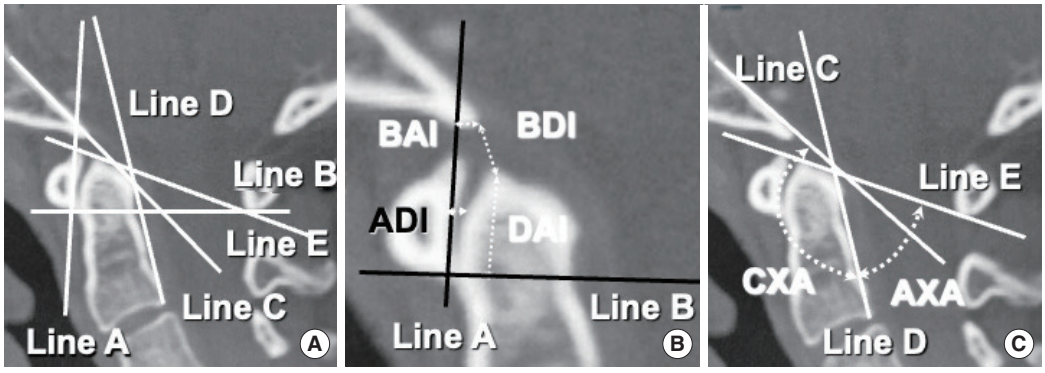

Fig. 3. Mporphometric measurement of craniocervical junction (CCJ) in the cases with hereditary disorders of connective tissue. (A) Two-dimension computed tomography (2D-CT) midline image of CCJ demonstrating reference lines. Line A means plane of the posterior surface of anterior arch of atlas. Line B means line between the lowest point of anterior arch of atlas and the lowest point of posterior arch of atlas. Line C means superior plane of the clivus. Line D means plane of posterior surface of the dens. Line E means plane of the top of anterior arch of atlas and the lowest point of posterior arch of atlas. (B and C) 2D-CT midline image demonstrating morphometric measurements. ADI, interval between anterior arch and dens; BAI, interval between basion and line A; BDI, interval between basion and top of dens; DAI, interval between top of dens and line B; AXA, angle between axis (line D) and atlas (line E); CXA, angle between clivus (line C) and axis (line D).

under intravenous anesthesia in the supine position and morphometric measurements were performed. Then, the patient was placed in an upright position and craniocervical instability was assessed on the basis of neurological symptoms, followed by repeat morphometric measurements. Cases with displacement of the occipito-atlanto-axial joints (>1.5 standard deviation [SD]) were defined as having instability. Craniocervical traction using 10–15 kg was applied, which resolved the neurological symptoms and led to a reduction of CCJ.

3. Statistical Analyses

The patient groups were compared with normal controls between groups divided into every 3 years old group. SPSS ver. 11.0 (SPSS Inc., USA) was used for statistical analyses. The means were compared between patients and normal controls using the Mann-Whitney U test. A p-value <0.01 was used to determine significance. For multiple analyses, heavy palindromic tests were used. Abnormalities of PCFV, VAFM, and occipital bone size were defined as values below 1.5 SD.

RESULTS: VOLUMETRIC AND MORPHOMETRIC ANALYSES OF PCF AND CCJ

The data along the development and growth in normal controls matched the previous reports.[24,25] Using multivariate regression analysis with PCFV, VAFM, and the size of the cartilaginous components of the occipital bone as explanatory variables, CM-I can be classified into 3 independent groups: CM-I types A, B, and C, and CM-borderline. The characteristics of these groups are summarized in Tables 1, 2 and Fig. 4.[16-18] CM-I types A (160 cases), B (156 cases), and C (131 cases). CM-borderline (37 cases) indicated borderline small occipital bone size and small VAFM (-1.0 to -1.5 SD).

1. Results of Volumetric and Morphometric Analyses of PCF and CCJ

PCFV was not significantly different between the cases and controls in all of age groups. Of the measured items, only PCFV, occipital bone size, and VAFM were significantly different between the cases and healthy controls. In CM-I type B, C and CM-borderline, PBFV/PCVF ratio in older than 4 years old age groups were signify larger than them in normal controls.

CM-I type A had normal PCFV, VAFM, and occipital bone size (Fig. 4A) in all of age groups. CM-I type B had normal PCFV, small VAFM and occipital bone size, large volume of PCFV above Twining line, and small PCFV below Twining line (Fig. 4B) in all of age groups. CM-I type C had small PCF, VAFM, and occipital bone size in all of age groups (Fig. 4C). In CM-I type A, MH was decreased and 4VH was increased compared to controls in older than 8 years old. In CM-I type C, MH was decreased and the position of 4VH was increased compared to controls in all of age groups since birth. CM-borderline had normal PCFV and occipital bone size, but borderline small VAFM after older than 8 years old (Fig. 4E).

https://doi.org/10.14245/ns.2551050.525

Table 1. Subtypes of CM-I classified based on the morphometric analyses, and the cause of hindbrain descent and surgical interventions

Variable	CM-I type A	CM-I type B	CM-I type C	CM- borderline
Occipital bone size	Normal	Small	Small	Small
PCFV	Normal	Normal	Small	Normal
VAFM	Normal	Small	Small	Small
PBFV/PCFV	Normal/large	Large	Large	Normal/large
Axial length of hindbrain	Normal	Normal	Elongation	Normal
Position of hindbrain	Downward displacement	Normal	Downward displacement	Normal
Cause	Others	Crowdedness of VAFM	Crowdedness of whole PCF	Crowdedness of VAFM
Intervention	Others	FMD	ESCP	FMD

CM-I, Chiari malformation type I; CM-borderline, Chiari malformation borderline; PCFV, volume of the posterior cranial fossa; VAFM, volume of area of surrounding foramen magnum; PBFV, volume of brain in the posterior cranial fossa; FMD, foramen magnum decompression; ESCP, expansive suboccipital cranioplasty.

Table 2. Other mechanisms of the brainstem and cerebellum in CM-I type A, CM-borderline, and surgical intervention including secondary hindbrain descent

Variable	Instability of CCJ	Tethering	Hydrocephalus	Intracranial mass/ macrocepahly	Pressure dissociation
PCFV	Normal	Normal	Normal	Normal	Normal
VAFM	Normal	Normal	Normal	Normal	Normal
PBFV/PCFV	Normal	Normal	Normal/large	Normal/large	Normal
Brainstem & cerebellum	Normal	Elongation and downward displacement		Normal/large	Normal
Cause	Cranial settling	Traction	Pressure coning		Hypotension of intraspinal canal
Intervention	CCF	Untethering/SFT	VPS	Resection of mass or FMD	Others

CM-I, Chiari malformation type I; CM-borderline, Chiari malformation borderline; CCJ, craniocervical junction; PCFV, volume of the posterior cranial fossa; VAFM, volume of area of surrounding foramen magnum; PBFV, volume of brain in posterior cranial fossa; CCF, craniocervical fixation; SFT, section of filumn terminale; VPS, ventriculo-peritoneal shunt; FMD, foramen magnum decompression.

2. Results of Morphometric Analyses of CCJ in Craniocervical Traction Test (Table 3)

The distance between anterior arch of atlas and dens (DAI) was used to evaluate the atlanto-axial horizontal dislocation. Change in ADI of >4 mm between flexion and extension is an accepted index of atlanto-axial horizontal dislocation.[16,18-23] The distance between dense and anterior arch of atlas (DAI) was used to evaluate the vertical basilar invagination. DAI>15 mm from the top of dens above McRae line is an accepted index of basilar invagination.[16,18-23] Furthermore, the morphometric analyses during craniocervical traction test revealed BDI (the distance between basion and top of dens), BAI (the distance between basion and anterior arch of atlas), and CXA (the angle between clivus and axial) as reliable and reproducible measurements in patients with instability of CCJ.

In the supine position, BDI, BAI, and CXA were normal. However, in the sitting position, the BDI decreased, BAI increased, and CXA decreased. During traction, these values returned to the normal range. In the follow-up evaluation of patients who underwent joint stabilization, normal values of BDI, BAI, and CXA were maintained. However, in patients without joint stabilization, these values were abnormal.

In 70 cases with instability, hereditary disorders of connective tissue was present in 28 cases, bony anomalies (including basilar invagination) in 43 cases and trauma in 18 cases. Out of CM-I type A, CM-I type B, CM-I type C, and CM- borderline, 58 (36.3%), 3 (1.9%), 5 (3.8%), and 4 (10.8%) had instability, respectively.

The cases with instability in CM-I type A were the most, there was significant more than other groups ($p<0.01$).

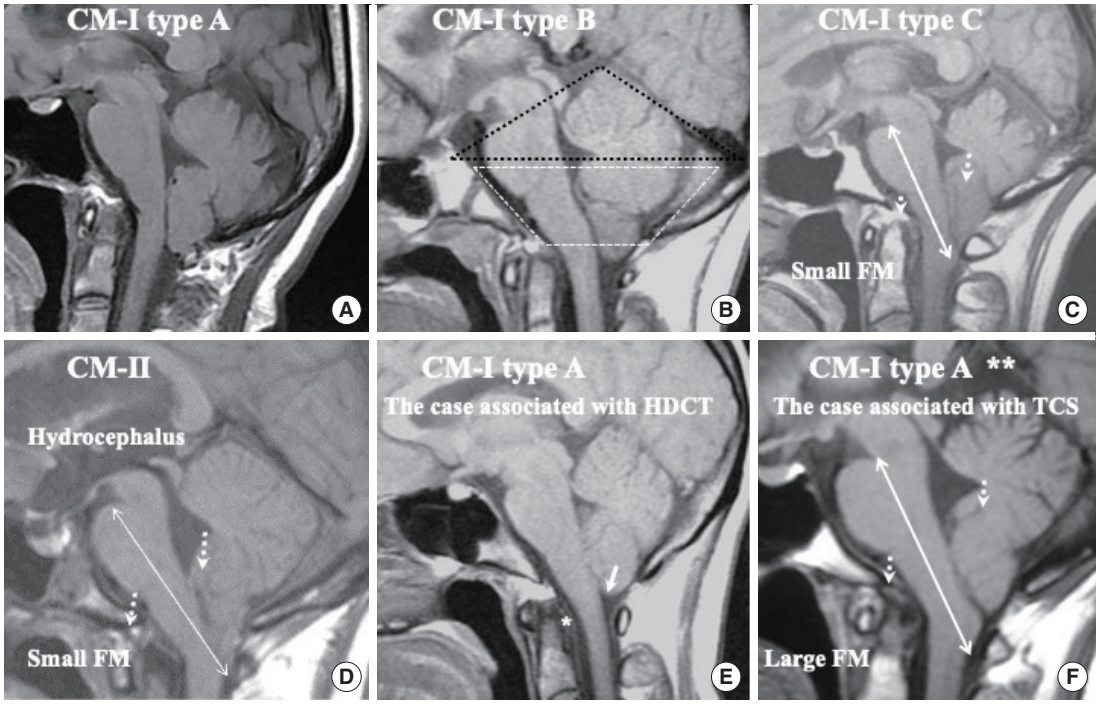

Fig. 4. Illustrative cases of Chiari malformation type I (CM-I) subtypes and Chiari malformation type II (CM-II). (A) CM-I type A: normal volume of the postrior cranial fossa (PCFV), normal volume of the surrounding area of foramen magnum (VAFM), normal occipital bone size. (B) CM-I type B: normal PFCV, small VAFM and occipital bone size, small of the volume of the below Twing's line (white doted trapezoid area) and compensatory expansion of the above Twing's line area (black doted trapezoid area). (C) CM-I type C: small PCFV, VAFM and occipital bone size, dowmward dispalcemet of the brain stem and cerebellum (doted arrows), elongation of the brain stem (white arrow). (D) CM-II: small PCFV, VAFM, and occipital bone size, downwad displacement of the btrain stem and cerebellum (white doted arrow) and elongation of the brain stem (white arrow). (E) CM-I type A: The case associated with hereditary disorders of connective tissue (HDCT): normal volume of the PCFV, normal VAFM, normal occipital bone size. Magnetic resonance (MR) midsagittal image in supine position showing normal BDI (7.7 mm), normal BAI (3.5 mm), normal CXA (141°), large retro-odontoid pannus (asterisk), and low-lying cerebellar tonsils. (F) CM-I type A: The case associated with tethered cord syndrome (TCS): mall PCFV, VAFM and occipital bone size, downwad displacement of the btrain stem and cerebellum (white doted arrow), elongation of the brain stem (white arrow) and large foramen magnum (FM). MR midsagittal image demonstrating the character of CM- I type A with TCS. PCFV, VAFM and occipital bone size are normal size. MR image shows elongation and downward displacement of the brain stem and cerebellum and large supuracerebellar cistern (double asterisk). BDI, the distance between basion and top of dens; BAI, the distance between basion and anterior arch of atlas; CXA, the angle between clivus and axial.

DISCUSSION

1. CM-I: Mechanism #1. Constriction of the PCF, CM-I Types B and C

To provide support for Mechanism #1, in which the PCF is abnormally small, resulting in the herniation of the hindbrain into the spinal cord, it is necessary to demonstrate that PCFV is reduced, while the volumes of the brainstem and cerebellum remain within normal limits. There are many reports which described that PCFV in CM-I is small.[26-32]

The total volume of the posterior fossa including the area enclosed by the cerebellar tentorium did not differ significantly from that of the control group, the volume of the portion bounded by the occipital bone and located caudal to Twining line was significantly reduced (Fig. 4B and C).[16-18] In contrast, the volumes of the brainstem and cerebellum were not significantly different compared to the normal group.[16-18]

Furthermore, how the narrowing of PCF in CM-I occurs from both anatomical and embryological perspectives was considered. According to reports by the anatomist, embryologist, and teratologist O'Rahilly, the occipital bone develops from 3 cartilaginous components, i.e., the basiocciput (clivus), exocciput (condyle), and supraocciput (convexity).[33-35]

 https://doi.org/10.14245/ns.2551050.525

Table 3. Results of morphometric measurements of craniocervical junction in craniocervical traction test

Variable	Normal controls (> 12 yr) (n = 30 cases)	Craniocervical test		During operation in positioning	Follow-up	
		Nontraction	Traction		CSJ cases	ICSJ cases
ADI (mm)						
Flexion position in sitting	3.40 ± 0.47	7.40 ± 1.24‡	3.30 ± 0.55	NA	3.40 ± 0.53	7.40 ± 1.24‡
Neutral position in sitting	2.80 ± 0.54	3.10 ± 0.63	3.00 ± 0.51	3.20 ± 0.45	3.00 ± 0.48	3.10 ± 0.63
Extension position in sitting	2.00 ± 0.48	2.30 ± 0.58	2.70 ± 0.47	NA	3.20 ± 0.52	2.30 ± 0.58
Supine position	2.80 ± 0.57	2.40 ± 0.34	2.50 ± 0.74	In positioning	2.20 ± 0.64	2.50 ± 0.52
Sitting position	2.40 ± 0.58	2.10 ± 0.42	1.94 ± 0.44	2.20 ± 0.78	2.40 ± 0.68	2.30 ± 0.64
BAI (mm)						
Supine position	1.80 ± 1.21	2.0 ± 1.25	2.20 ± 1.52	In positioning	2.20 ± 1.30	2.50 ± 1.48
Sitting position	2.10 ± 1.88	5.10 ± 1.22‡	1.85 ± 0.71	2.00 ± 1.21	2.30 ± 1.38	5.30 ± 1.57‡
BDI (mm)						
Supine position	7.40 ± 1.58	8.70 ± 1.70	8.80 ± 2.23	In positioning	8.30 ± 1.82	7.60 ± 2.01
Sitting position	7.20 ± 1.59	3.90 ± 1.81†	8.40 ± 2.20	8.70 ± 2.70	8.20 ± 1.84	3.80 ± 1.92†
AXA (°)						
Supine position	37.60 ± 6.55	35.20 ± 5.44	4.72 ± 6.23	In positioning	34.50 ± 6.04	35.30 ± 5.43
Sitting position	37.40 ± 6.84	36.50 ± 5.96	35.80 ± 5.88	36.70 ± 6.40	35.40 ± 5.44	34.40 ± 5.41
CXA (°)						
Supine position	147.60 ± 6.61	145.20 ± 5.27	146.50 ± 5.68	In positioning	144.80 ± 5.49	145.80 ± 5.58
Sitting position	147.80 ± 6.00	136.80 ± 6.47†	145.40 ± 5.88	146.80 ± 6.45	145.20 ± 5.58	134.20 ± 5.58†

Values are presented as mean ± 1 standard deviation.
CSJ, complete stabilization of joints; ICSJ, incomplete stabilization of joints; ADI, the distance between atlas and dens; BAI, the distance between basion and anterior arch of atlas; BDI, the distance between basion and top of dens; AXA, the angle between atlas and axis; CXA, the angle between clivus and axial; NA, not applicated.
†Significantly smaller than those of normal controls ($p < 0.01$). ‡Significantly larger than those of normal controls ($p < 0.01$).

1) Neuroradiological considerations

Morphometric measurements were performed on the neuroradiological images. These 3 parts (clivus, condyle, and supraocciput) of the occipital bone were measured using x-ray and computed tomography scans from patients,[16-18] and all were found to be hypoplastic.

Moreover, as the cerebellar tentorium steepened, it compensated for the narrowing of the bony elements caudal to Twining line, resulting in no significant difference in the overall volume of the PCF compared to control groups (Fig. 4B and C).[16-18] This phenomenon was named "remodeling of the posterior fossa." However, the ratio of the PCF volume to the volumes of the brainstem and cerebellum—as proposed in Hypothesis #1—was indicated a constricted PCF.[16-18]

2) Experimental considerations

Marin-Padilla and colleagues reported that the excessive administration of retinoic acid to pregnant hamsters induced encephalocele and Chiari malformation in their fetuses.[36-49] Morphological measurements of the occipital bone, brainstem, and cerebellum were conducted in these specimens. Retinoic acid affected the expression of Hox genes, which regulate region-specific morphological differentiation, leading to backward displacement.[40-44]

This morphological transformation of the vertebrae resulted in severe malformations of the occipital bone—located at the most cranial end and at the craniovertebral junction. In contrast, excessive retinoic acid exposure led to encephalocele, herniation of the hindbrain into the spinal canal (Chiari malformation), and severe malformation of the cranial base derived from the paraxial mesoderm.[40-44] The details of this phenomenon were described, including genetic analysis.

3) Skull base abnormalities in the context of embryological mesodermal defects

Patients with CM-I of the atlas, axis, and/or subaxial cervical vertebrae include those with Klippel-Feil deformity, complete or partial atlanto-occipital assimilation, and hypoplasia, dyspla-

sia, or agenesis of the atlas, among others. These findings support a mesodermal disorder and abnormal segmentation of the somite-derived cervical vertebral bodies as underlying causes of CM-I.[45,46] Such bony anomalies likely contribute to the narrowing of the PCF.

4) Genetic research: insufficiency of PCF development

Marin-Padilla and Marin-Padilla demonstrated one potential mechanism for CM-like development using a hamster model.[36-39] Additionally, CM-I has been reported in patients with mutations in retinoic acid receptor beta.[47] Retinoic acid, a metabolite of dietary vitamin A, plays multiple roles in embryonic development and cellular differentiation.[48,49] Furthermore, retinoic acid regulates fibroblast growth factor (FGF) signaling during development.[50] Similarly, gain-of-function mutations in FGF receptor 3 result in defects in posterior fossa morphology in mouse models, including alterations in the shape and size of the foramen magnum.[51] FGF receptor mutations are also linked to disorders such as craniosynostosis and achondroplasia.

Craniosynostosis, the premature closure of one or more sutures between the skull plates, is often linked with CM-I.[26] It can occur as part of syndromes that are also associated with CM-I, such as Crouzon syndrome.[26] Specifically, recurrent mutations affecting FGF signaling in craniosynostosis may also contribute to CM-I.

Beyond retinoic acid and FGF signaling, other genes involved in related developmental processes may play a role. At least 7 individual cases of mutations in the ETS2 repressor factor gene have been associated with CM-I and craniosynostosis.[51] ETS2 repressor factor may act downstream of FGF signaling during mesodermal induction.[52] A small posterior fossa may also be linked to other craniocervical bone anomalies, such as occipital dysplasia, commonly resulting in an underdeveloped occipital bone and reduced posterior fossa size.[17,29]

Recently, Brockmeyer et al.[53] built on data from Abbott et al.[54] using the Utah Population Database to identify a candidate variant in homeobox C4 that may affect the development of the junction between the mesoderm and neural crest, leading to a decreased clivo-axial angle and CM-I. Matsuoka et al.[55] proposed that widening of the foramen magnum, caused by post-otic neural crest–derived mesenchymal stem cells being respecified from bone to connective tissue, may also contribute to CM-I.

2. CM-I: Mechanism #2, CM-I Type A

Embryogenic growth dysregulation is a rare disorder that results in the overgrowth of multiple somatic tissues, including the central nervous system. Macrocerebellum is characterized by an abnormally large cerebellum with preserved overall morphology[56,57] Evaluation of cerebellar architecture in these disorders reveals that the cerebellar hemispheres are enlarged due to increased cerebellar gray matter.[58] A developmental excess of neural tissue within a normal-sized posterior fossa may cause the cerebellar tonsils to descend. In this case, PBFV is large, but occipital bone size, PCFV are normal, and so PBFV/PBFV is large. Therefore, these cases were classified into CM-I type A.

In macrocephaly-capillary malformation syndrome, approximately 50% of patients exhibit progressive tonsillar descent associated with rapid brain growth and increased crowding of the posterior fossa during infancy.[58] In a longitudinal study of 67 patients, Conway et al.[58] found that although newborns had normal cerebellar size, they developed cerebellar overgrowth and tonsillar descent during the first year of life, despite normal posterior fossa volume. Therefore, in these syndromes, cerebellar overgrowth results in a structural mismatch between the skull and neural tissue.

3. CM-I: Mechanism #3, CM-I Type A

Mechanism #3 proposes that the brainstem and cerebellum are pulled downward from below (caudally), resulting in their herniation, e.g., tethered cord syndrome and CM-II.

Milhorat, Bolognese, and Nishikawa reported Chiari malformation in patients with tethered cord syndrome.[59,60] In several cases, sectioning of the filum terminal resulted in an upward shift of the brainstem and cerebellum. They also documented cases of occult tethered cord syndrome and scoliosis associated with Chiari malformation, in which sectioning of the filum terminal led to an improvement in brainstem and cerebellar descent. Surgical outcomes were reported and published.[59,60]

Although circumstantial evidence has accumulated, the traction hypothesis (hypothesis #3) remains unproven. Animal studies involving cats and dogs have been conducted, but when slight tension was applied to the caudal lumbar nerve roots, the brainstem and cerebellum did not descend, likely due to the elasticity of the spinal cord.

In contrast, in CM-II, the brainstem and cerebellum descend caudally from the fetal stage, presumably due to traction from a meningocele in combination with hydrocephalus (Fig. 4C).[36-39,61]

4. CM-I: Mechanism #4, CM-I Type A

1) Neuroradiological considerations

Milhorat, Bolognese, and Nishikawa reported patients with hereditary connective tissue disorders who experienced symp-

 https://doi.org/10.14245/ns.2551050.525

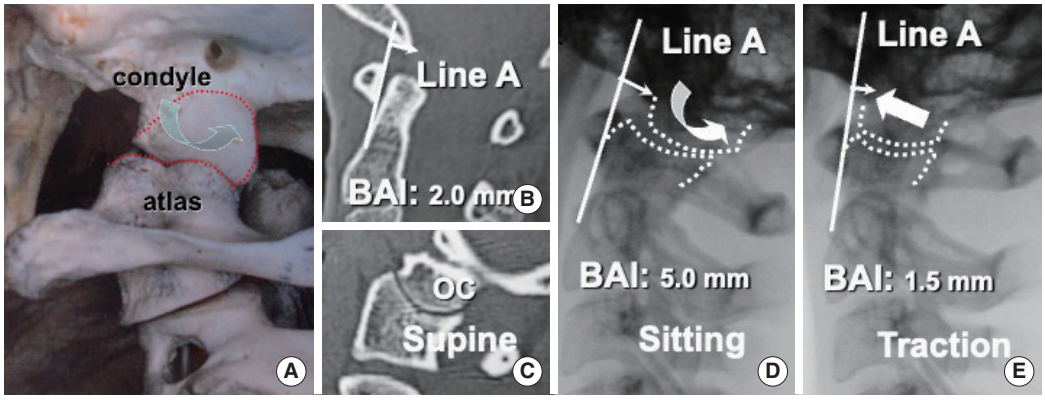

Fig. 5. Morphometric measurement of craniocervical junction in the cases with hereditary disorders of connective tissue. (A) Photo showing the bony model of left occipitto-atlantal joint. The occipital condyle glides to posterior against atlas on sitting position. Red dotted line: the margin of atlanto-occipital joint. Blue arrow: posterior gliding and anterior flex of the occipital condyle. (B and C) The results midsagittal reconstructed 2-dimension computed tomography scanning with the patient in the supine position, showing BAI of 2.0 mm (lower left) and normal articulation of occipital condyle (OC) (lower left). (D and E) The results plain radiography showing an increase of BAI (5.0 mm) in the sitting position and a decrease of BAI (1.5 mm) during traction with a 20-lb (9.1 kg) weight. The occipito-atlantal joint (outline by dotted line) glides posteriorly in the sitting position (curved arrow) and its reduced by traction (straight arrow). Line A, plain of the posterior surface of the anterior arch of the atlas.

toms such as dizziness, limb numbness, swallowing difficulties, and shortness of breath when sitting or standing.[62,63] These symptoms were relieved by traction. Using open MRI, these cases were examined in the sitting position. While these phenomena did not occur in the supine position, the cerebellar tonsils were found to descend into the spinal canal when the patients were seated (Fig. 5), which was termed "cranial settling." In these patients, the volume of the PCF and size of the cartilaginous components of the occipital bone were within normal ranges. Morphological measurements revealed "cranial settling" and a "posterior gliding" phenomenon (Fig. 5), in which the occipital condyles slid backward relative to the atlanto-occipital joint. Upon applying cranial traction, these neurological symptoms disappeared, and measurements showed. This condition of at the occipito-atlas-axis joints was observed frequently in patients with hereditary connective tissue disorders, as the pilot data were reported by Milhorat, Bolognese, and Nishikawa.[62,63]

2) Genetic research: insufficiency of connective tissue

In addition to the skull, connective tissue plays a crucial role in supporting the cerebellum. Boyles et al.[64] performed linkage analysis on 23 families with 71 affected individuals. Of the 10,000 single nucleotide polymorphisms analyzed, they identified possible associations with chromosomal regions 15q21.1–22.3 and 9q21.33–33.1.[64] The 15q21.1–22.3 region contains the fibrillin 1 gene, which is linked to Marfan syndrome and Shprintzen-Goldberg syndrome, both known to co-occur with CM-I.[65] Other connective tissue disorders, such as Ehlers-Danlos syndrome type 3 (hypermobility type), Loeys-Dietz syndrome, Stickler syndrome, and self-identified hypermobility, have also been associated with CM-I.[65,66] These associations may be related to increased tissue mobility and decreased stability, which could facilitate cerebellar herniation. Mutations in collagen type IV alpha 1 chain have likewise been associated with CM-I.[67]

DECISION OF SURGICAL INTERVENTIONS: ALGORITHM FOR CHOOSING SURGICAL INTERVENTION AND TREATMENT TO ASSOCIATED SYRINGOMYELIA

1. Algorithm for Choosing Surgical Intervention

We propose the algorism for surgical; intervention, the important measurements are the occipital bone size, PCFV and VAFM (Fig. 6).

The primary goal of surgical treatment for Chiari malformations and its related disorders is decompression of the brainstem and cerebellum, as well as the resolution and normalization of cerebrospinal fluid (CSF) flow obstruction at the foramen magnum. To achieve these goals, fundamental surgical intervention must address the underlying pathogenesis and mechanisms of hindbrain descent. Therefore, we selected foramen magnum decompression (FMD) for CM-I type B and CM-borderline, because VAFM and occipital bone size were small in these pa-

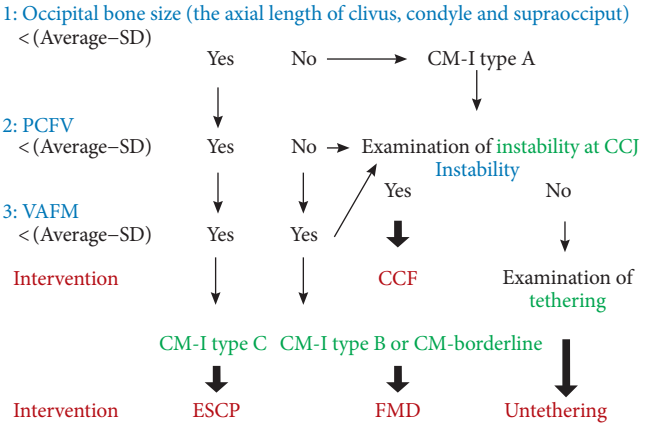

Fig. 6. Algorithm for descicion of surgical management. Blue words: morohometric parameters for classification, Green words: the pathogenesis/mechanism of hindbrain descent, Red words: surgical intervention. SD, standard deviation; CM-I, Chiari malformation type I; PCFV, the volume of the posterior cranial fossa; VAFM, the volume of foramen magnum; CCF, cranioicervical fixation; ESCP, expansive suboccipital cranioplasty; FMD, foramen magnum decompression.

tients.[68] The authors suggested that FMD is adequate for CM-I type B and CM-borderline with small VAFM but normal PCFV. Conversely, in CM-I type C, it is necessary to expand the entire PCF and remodel the relationship between the brain and occipital bone. According to Sakamoto et al.,[69] we selected expansive suboccipital cranioplasty (ESCP) for CM-I type C because FMD was not adequate under the setting of small VAFM, small PCFV, and small occipital bone size. In CM-I type A, other surgical methods that can treat ptosis of the brainstem and cerebellum must be selected. Craniocervical posterolateral fixation (CCF) should be selected for cases with CCJ instability causing functional cranial settling.[19,62,70-72] Initially, it is important to identify the CCJ with instability. Next, it is important to select the appropriate methods of screw insertion. The most important anchor for screw insertion is C2 and pedicle screw for C2 is the ideal.

2. Surgical Intervention to Syringomyelia Associated With CM-I

Among the disorders associated with Chiari malformation, syringomyelia is the most common and clinically significant condition. In cases of syringomyelia, obstruction of CSF flow at the foramen magnum—caused by hindbrain descent, as seen in CM-I—is considered to be the main pathophysiological mechanism.[73,74] Clinically, the main symptoms are spinal cord-related due to syringomyelia, but neurological symptoms resulting from compression of the brainstem and cerebellum, such as cranial nerve palsies and headaches due to CSF flow disturbances, are also frequently observed.

MATERIALS AND METHODS: SURGICAL INTERVENTION FOR CM-I, CM-BORDERLINE, AND INSTABILITY

1. Surgical Indications and Patient Population

Surgery was performed in cases of myelopathy, upper cervical cord symptoms, brainstem symptoms, and Japanese Orthopaedic Association (JOA) score < 14.[75]

In total, 484 patients underwent surgical treatment: 302 underwent FMD, 104 underwent ESCP, and 70 underwent CCF. 10 patients underwent ventricle peritoneal shunt and 10 underwent section filum terminal and/or lysis of adhesion of the spinal cord.

Patient group for surgical interventions was same as that for the volumetric and morphometric study. The patients were treated between April 2006 and March 2020 at the institute or hospitals as described above.

2. Operative Procedures for CM-I Types B and C, and CM-Borderline

FMD consists of craniectomy of the surrounding area of the foramen magnum (2–3-cm square), decompression of the brainstem and cerebellum, and creation of major cisterns and flow out of CSF from the foramina of Magendie and Luschka.[68] ECSP involves extensive decompression to expand the surrounding area of foramen magnum and the entire PCF (along the transverse sinus and sigmoid sinus), C1 laminectomy, dural plasty, and osteoplasty to maintain the PCF expansion.[69] ESCP can achieve normalized PCFV and major cisterns, which is adequate for the decompression of the brainstem and cerebellum, and to remodel the appropriate positional relationship between the brainstem, cerebellum, and occipital bone by expanding the entire PCF, including C1.

In children younger than 12 years, the cranium and brain are under development, so the possibility of disproportion between the cranium and brain changes over time. For patients younger than 12 years, FMD was performed first.

3. Operative Procedures for CM-I Type A and Instability

CCF was performed for CCJ instability.[19,70] If the patient had instability at CCJ joints, occipitocervical posterolateral fixation (OCF) should be performed. For patients with instability at the

https://doi.org/10.14245/ns.2551050.525

atlanto-axial joints alone, C1–2 posterolateral fixation (C1–2 FIX) should be performed. In cases where pedicle screw could be inserted for C2, fixation of C2 with screws was adequate. In cases where screw insertion was not possible, it was necessary to fix C2 to C3 or C4.

CCF was performed in a total of 70 cases, of which C1–2 FIX was performed in 36 cases and OCF in 34 cases. For cases (7 cases) with CCJ instability associated with CM-I types B and C, and CM-borderline, staged CCF combined with ESCP or FMD was performed.

In children younger than 12 years, the relationships between the anatomical structures are under development, so there is a possibility of overestimating the instability. In children, the loss of function of occipito-atlanto-axial joints induces significant handicap. Therefore, CCF was not performed in children younger than 12 years.

4. Neurological and Neuroradiological Examinations, Follow-up, and Statistical Analyses

Postoperatively, the neurological symptoms and signs, JOA score, recovery rate of JOA score[75] (JOA score RR) ([postoperative points–preoperative points]/[full points–preoperative point] × 100%) , and neuroradiological findings (cervical spine dynamic x-ray, 2D-CT, and MRI of the cervical spine) were examined every 3 months. Persistent syringomyelia was defined by confirmation of syringomyelia larger than 2 mm in diameter. Surgical outcome was assessed using chi-square and Fisher tests. A p-value <0.01 was used to determine significance.

RESULTS: SURGICAL INTERVENTION FOR CM-I, CM-BORDERLINE, AND INSTABILITY

The follow-up duration was 24–216 months (mean, 88.5 months). The results were based on the most recent data. In total, 58 patients were lost to follow up after more than 3 years of operation, in whom, the results of the final examination were estimated.

1. Results of JOA Score and RR in FMD and ESCP (Table 4)

In 12 and older than 12 years old adolescence and adult cases, the improvement rate of neurological symptoms and signs in FMD was 87.8%. The JOA score RR in FMD was 58.7 %, while 92.2% of cases showed improvement or stabilization of neurological symptoms. In 14 cases (7.8%), the neurological symptoms deteriorated during follow-up. In 10 cases out of 127 cases (7.9%) with syringomyelia, the symptoms persisted. The improvement rate of neurological symptoms and signs in ESCP was 88.2%. The JOA score RR in ESCP was 60.2%, and 98.0% of cases had an improvement or stabilization of neurological symptoms. In 2 cases (2.0%), the neurological symptoms deteriorated during follow-up. In 1 case out of 38 cases (2.6%) with syringomyelia,

Table 4. JOA score and its recovery rate after FMD and ESCP

Variable	Improved neurological symptoms/signs	JOA score RR (%)	Resyringomyelia	Stabilized neurological symptoms/signs	Deteriorated neurological symptoms/signs	Transient morbidities
Total number: 404 cases	339/404 (83.9)	58.5 ± 10.4	21/221 (9.5)	24/404 (5.9)	42/404 (10.4)	10/404 (2.5)
12 Years or older (≥ 12 yr)						
FMD (n = 180) (for CM-I types A, B and CM-borderline)	158/180 (87.8)	58.7 ± 10.2	10/127 (7.9)†	8/180 (4.4)	14/180 (7.8)†	3/180 (1.7)
ESCP (n = 102) (for CM-I type C)	90/102 (88.2)	60.2 ± 10.1	1/38 (2.6)	10/102 (9.8)	2/102 (2.0)†	4/104 (3.9)†
Younger than 12 yr (< 12)						
FMD for all types (n = 122)						
CM-I type A (n = 45)	31/45 (68.9)‡	57.2 ± 9.1	4/12 (33.3)†	0/45 (0)	14/45 (31.1)†	1/45 (2.2)
CM-I type B (n = 41)	34/41 (80.5)	58.2 ± 10.1	1/30 (3.3)	5/41 (12.2)	2/41 (4.2)	1/41 (2.4)
CM-I type C (n = 29)	20/29 (69.0)‡	48.6 ± 10.2‡	5/10 (50.0)†	0/29 (0)	10 /29 (34.5)†	1/29 (3.4)
CM-borderline (n = 7)	6/7 (85.7)	54.3 ± 10.4	0/4 (0)	1/7 (14.2)	0/7 (0)	0 /7 (0)

Values are presented as number (%) or mean ± 1 standard deviation.
JOA, Japanese Orthopaedics Association; FMD, foramen magnum decompression; ESCP, expansive suboccipital cranioplasty; RR, recovery rate; Resyringomyelia, syringmyelia remaining; CM-I, Chiari malformation type I; CM-borderline, the cases which have neurological brain stem and/or myelopathy; but tonsillar herniation less than 5 mm.
†Significantly higher or more than other groups ($p<0.01$). ‡Significantly lower or less than other groups ($p<0.01$).

Table 5. JOA score and its recovery rate after craniocervical fixation

Operative procedure	Improved neurological symptoms/signs	Preop JOA score	Postop JOA score	JOA score RR (%)	Bony fusion of joints	Stabilization of joints
CCF (n = 70 cases)	65/70 (92.9)	4–12 (9.7 ± 2.48)	10–17 (15.5 ± 2.51)	69.7	47/70 (67.1)	59/70 (84.3)
C1–2 FIX (n = 36 cases)	34/36 (94.4)	4–12 (9.0 ± 2.55)†	14–17 (15.4 ± 2.58)	78.7†	26 /36 (72.2)†	32/36 (88.9)†
OCF (n = 34 cases)	32/34 (94.1)	3–12 (6.4 ± 2.43)‡	10–17 (15.7 ± 2.48)	63.5‡	21/34 (61.8)‡	27/34 (79.4)‡

Values are presented as number (%) or mean ± 1 standard deviation (range).
JOA, Japanese Orthopaedics Association; Preop, preoperative; RR, recovery rate; CCF, craniocervical fixation; C1–2 FIX, atlanto-axial posterior lateral fixation; OCF, occipitocervical fixation.
†Significantly higher than OCF ($p < 0.01$). ‡Significantly lower than C1/2 FIX ($p < 0.01$).

the symptoms persisted. There was no significant difference between the FMD and ESCP groups in terms of improvement or stabilization of neurological symptoms and the JOA score RR. Persistent syringomyelia and deteriorated cases of neurological symptoms and/or signs were significantly more common in patients who underwent FMD compared to ESCP ($p > 0.01$).

In younger 12 years old child, improvement rate of neurological symptoms and/or signs were significantly lower in CM-I types A (68.9%) and C (69.0%) than them in CM-I type B (80.5%) and CM- borderline (85.7%) ($p > 0.01$). JOA score RR was significantly lower in CM-I type C (48.6%) than them in CM-I types A (57.2%), B (58.2%), and CM- borderline (54.3%) ($p > 0.01$). Persistent syringomyelia and deteriorated cases of neurological symptoms and/or signs were significantly more common in patients of CM-I types A (33.3%, 31.1%) and C (50.0%, 34.5%) in patients of CM-B (3.3%, 4.2%) and CM-borderline (0%, 0%) ($p > 0.01$).

2. Results of JOA Score and RR in CCF (Table 5)

The JOA score RR among the 70 cases who underwent CCF was 69.7%. In total, 46 cases (67.1%) had complete bony fusion, 59 cases (84.3%) had stabilized joints, and 11 cases (15.7%) had incomplete stabilization. Syringomyelia resolved in all 21 cases.

Preoperative JOA score in C1–2 FIX was significantly lower than that in OCF. In 36 cases who underwent C1–2 FIX, the JOA score RR was 78.7%. In total, 26 cases (72.2%) had complete bony fusion, 32 cases (88.9%) had stabilized joints, and 4 cases (11.1%) had incomplete stabilization. The JOA score RR in the 34 cases who underwent OCF was 63.5%. In total, 21 cases (61.8%) had complete bony fusion, 27 cases (79.4%) had stabilized joints, and 7 cases (20.6%) had incomplete stabilization. In cases who underwent C1–2 FIX, the JOA score RR, rate of stabilization, and bony fusion of joints was higher than those in cases who underwent OCF.

3. Complications and Side Effects

In the FMD and ESCP groups, there was no mortality or permanent morbidity. Transient morbidity occurred in 10 cases (2.5%). Complications were observed in 6 cases (2.6%) with FMD and 4 cases (3.8%) with ESCP. Two cases (0.7%) with FMD had wound infection, in 2 case (0.7%), in 1 case (0.3%) with FMD had arachnoid adhesion, in 1 case (0.3%) with FMD had CSF leakage. Two cases (3.8%) with ESCP had wound infection, in 1 case (1.0%), cerebellar slugging occurred without neurological symptoms, in 1 case (1.0%) with ESCP had CSF leakage. Repetitive and persistent neck pain continued in 3 cases (2.9%) with ESCP. There were significantly more complications and side effects in ESCP than FMD.

In both C1–2 FIX and OCF, there was no mortality or permanent morbidity. Transient morbidity occurred in 2 cases (2.9%). The complications included transient swallowing disturbance in 1 case (1.4%) in OCF and injury to the vertebral artery without neurological symptoms in 1 case (1.4%) in C1–2 FIX. Repetitive and persistent neck pain continued in 3 cases (8.8%) of OCF and functional loss of visual fields occurred in 2 cases (5.9%). There were significantly more complications and side effects in OCF than C1–2 FIX.

DISCUSSION: CLINICAL IMPACT BY APPLICATION OF THE NEW CLASSIFICATION SYSTEM

Compared to previous reports involving only FMD, our results showed improved outcomes with fewer reoperations. In particular, the improvement rate for brainstem compression symptoms was markedly better, suggesting effective brainstem decompression and normalization of CSF flow dynamics. When posterior fossa narrowing is confined to the foramen magnum region, FMD alone appears sufficient for decompression and CSF flow restoration. Additionally, morbidity and complication

https://doi.org/10.14245/ns.2551050.525

rates were lower in our cohort.[76-79] These findings support the appropriateness of selecting the surgical procedure (ESCP or FMD) based on morphometry.[80-82]

C1–2 FIX and OCF both resulted in high rates of neurological symptom improvement, joint stabilization, and/or bony fusion.[80-84] Our outcomes surpassed those of previous reports, supporting the effectiveness of CCF in managing "cranial settling" and "posterior gliding" due to CCJ instability/hypermobility. However, OCF was associated with greater functional loss and more frequent complications due to fixation of the occipito-atlanto-axial joints than C1–2 FIX. Thus, fixation involving the occipital bone requires careful consideration. The CCJ at traction test has proved useful in detecting occipito-atlanto-axial instability/hypermobility and assessing the risks of functional loss after fixation.[80-82]

CONCLUSIONS

We reviewed 4 existing hypotheses regarding the causes of hindbrain descent, along with the supporting studies for each. Through morphological measurements of PCF and CCJ, we were able to infer the mechanisms and pathogenesis of hindbrain descent. This contributes to the selection of appropriate surgical treatment strategies.

Morphological differences are considered phenotypes of the underlying genes. On the basis of morphological measurements and analyses of PCF, CCJ, hindbrain, Chiari malformation can be classified according to its causes. Many diseases involving hindbrain descent, as well as malformations and instability of the CCJ, are believed to originate during fetal development or even earlier at the genetic level.

As studies continue to reveal an increasing number of potential pathogenic associations, further approaches to understand the functional consequences of gene variants will be essential. We anticipate continued advances in our understanding of the genetics and etiology of CM-I, which we hope will lead to improved treatment selection and better clinical care for patients with CM-I.

NOTES

Conflict of Interest: The authors have nothing to disclose.

Funding/Support: This study received no specific grant from any funding agency in the public, commercial, or not-for-profit sectors.

Acknowledgments: The authors deeply thank Professor Emeritus Thomas H. Milhorat, M.D., Feinstein Institutes for Medical Research, Northwell Health, Manhasset, New York, for leading this review and proving support.

Research Ethics: This review has approved by the Institutional Review Board of Osaka Metropolitan University (OMH-2018-4243) and Moriguchi Ikuno Memorial Hospital (MIMH-2018-1). A written informed consent should be obtained from all subjects.

Author Contribution: Conceptualization: MN, PAB; Formal analysis: HS, MH; Investigation: MN, MY, KN, NK, HI; Methodology: MN, MY, KN, NK; Project administration: MN, TG; Writing – original draft: MN, PAB; Writing – review & editing: MN, TG, MH, KO.

ORCID

Misao Nishikawa: 0000-0002-0808-390X
Paolo A. Bolognese: 0000-0002-5207-7232
Kentarou Naito: 0000-0002-1847-7064
Kenji Ohata: 0000-0001-7334-8321

REFERENCES

1. Chiari H. Über veränderungen des kleinhirns, des pons und der medulla oblongata in folge von congenitaler hydrocephalie des grosshirns. Wien (Austria): K.K. Hof- und Staatsdruckerei; 1895. p. 71-116.
2. Chiari H. Über veränderungen des kleinhirns infolge von hydrocephalie des grosshims. Dtsch Med Wochenschr 1891;17:1172-5.
3. Arnold J. Myelocytes, transposition von gewebskeimen und Sympodie. Beitr Pathol Anat 1894;16:1-28.
4. Ciaramitaro P. Garbossa D. Peretta P, et al. Syringomyelia and Chiari syndrome registry: advances in epidemiology, clinical phenotypes and natural history based on a North Western Italy cohort. Ann Ist Super Sanita 2020;56:48-58.
5. Tubbs RS, Turgut M. Defining the Chiari malformations: past and newer classifications. In: Tubbs RS, Turgut M, Oakes WJ, editors. The Chiari malformations. 2nd ed. New York: Springer; 2020. p. 21-39.
6. Aboulezz A, Sartor K, Geyer CA, et al. Position of cerebellar tonsils in the normal population and in patients with Chiari malformation: a quantitative approach with MR imaging. J Comput Assist Tomogr 1985;9:1033-6.
7. Barkovich A, Wippold FJ, Sherman JL, et al. Significance of cerebellar tonsillar position on MR. AJNR Am J Neuroradiol 1986;7:795-9.

8. Elster AD, Chen MY. Chiari I malformations: clinical and radiological reappraisal. Radiology 1992;183:347-53.
9. Bogdanov EI, Iaizutdinova AT, Heiss JD, The small posterior cranial fossa syndrome and Chiari malformation type 0. J Clin Med 2022;11:5472.
10. Chern JJ, Gordon AJ, Mortazavi MM, et al. Pediatric Chiari malformation type 0: a 12-year institutional experience. J Neurosurg Pediatr 2011;8:1-5.
11. Iskandar BJ, Hedlund GL, Grabb PA, et al. The resolution of syringohydromyelia without hindbrain herniation after posterior fossa decompression. J Neurosurg 1998;89:212-6.
12. Morgenstern PF, Tosi U, Uribe-Cardenas R, et al. Ventrolateral tonsillar position defines novel Chiari 0.5 classification. World Neurosurg. 2020 Apr;136:444-53.
13. Tubbs RS, Elton S, Grabb P, et al. Analysis of the posterior fossa in children with the Chiari 0 malformation. Neurosurgery 2001;48:1050-4; discussion 1054-5.
14. Tubbs RS, Iskandar BJ, Bartolucci AA, et al. A critical analysis of the Chiari 1.5 malformation. J Neurosurg 2004;101(2 Suppl):179-83.
15. Tubbs RS, Turgut M, Oakes WJ. A history of the Chiari malformations. In: Tubbs RS, Turgut M, Oakes WJ, editors. The Chiari malformations. 2nd ed. New York: Springer; 2020. p. 3-20.
16. Milhorat TH, Nishikawa M, Kula RW, et al. Mechanisms of cerebellar tonsil herniation in patients with Chiari malformations as guide to clinical management. Acta Neurochir (Wien) 2010;152:1117-27.
17. Nishikawa M, Sakamoto H, Hakuba A, et al. Pathogenesis of Chiari malformation: a morphometric study of the posterior cranial fossa. J Neurosurg 1997;86:40-7.
18. Nishikawa M, Bolognese PA, Kula RW, et al. Pathogenesis and classification of Chiari malformation type i based on the mechanism of ptosis of the brain stem and cerebellum: a morphometric study of the posterior cranial fossa and craniovertebral junction. J Neurol Surg B Skull Base 2021;82:277-84.
19. Goel A, Gore S, Shah A, et al. Atlantoaxial fixation for Chiari 1 formation in pediatric age-group patients: report of treatment in 33 patients. World Neurosurg 2018;111:e668-77.
20. Ranawat CS, O'Leary P, Pellicci P, et al. Cervical spine fusion in rheumatoid arthritis. J Bone Joint Surg Am 1979;61: 1003-10.
21. Harris JH Jr, Carson GC, Wagner LK. Radiologic diagnosis of traumatic occipitovertebral dissociation: 1. Normal occipitovertebral relationships on lateral radiographs of supine subjects. AJR Am J Roentgenol 1994;162:881-6.
22. Harris JH Jr, Carson GC, Wagner LK, et al. Radiologic diagnosis of traumatic occipitovertebral dissociation: 2. Comparison of three methods of detecting occipitovertebral relationships on lateral radiographs of supine subjects. AJR Am J Roentgenol 1994;162:887-92.
23. Smoker WR. Craniovertebral junction: normal anatomy, craniometry, and congenital anomalies. Radiographics 1994; 14:255-77.
24. Hoyte DAN. Growth of the cranial base in human. In: Dexon AD, Hoyte DAN, Ronning O, editors. Fundamentals of craniofacial growth. New York: CRC press; 1997. p. 278-91.
25. Sgouros S, Kountouri M, Natarajan K. Posterior fossa volume in children with Chiari malformation Type I. J Neurosurg 2006;105(2 Suppl):101-6.
26. Cinalli G, Spennato P, Sainte-Rose C, et al. Chiari malformation in craniosynostosis. Childs Nerv Syst 2005;21:889-901.
27. Krogness KG. Posterior fossa measurements. I. The normal size of the posterior fossa. Pediatr Radiol 1978;6:193-7.
28. Krogness KG, Nyland H. Posterior fossa measurements. II. Size of the posterior fossa in myelomeningocele. Pediatr Radiol 1978;6:198-202.
29. Milhorat TH, Chou MW, Trinidad EM, et al. Chiari I malformation redefined: clinical and radiographic findings for 364 symptomatic patients. Neurosurgery 1999;44:1005-17.
30. Nyland H, Krogness KG. Size of posterior fossa in Chiari type 1 malformation in adults. Acta Neurochir (Wien) 1978;40: 233-42.
31. Stovner LJ, Bergan U, Nilsen G, et al. Posterior cranial fossa dimensions in the Chiari I malformation: relation to pathogenesis and clinical presentation. Neuroradiology 1993;35: 113-8.
32. Vega A, Quintana F, Berciano J. Basichondrocranium anomalies in adult Chiari type I malformation: a morphometric study. J Neurol Sci 1990;99:137-45.
33. Hamilton W. Mossman's human embryology: prenatal development of form and function. Hoffer (UK): Cambridge; 1972.
34. Maschner A, Krück S, Draga M, et al. Developmental dynamics of occipital and cervical somites. J Anat 2016;229:601-9.
35. O'Rahilly R, Müller F, Meyer DB. The human vertebral column at the end of the embryonic period proper. 2. The occipitocervical region. J Anat 1983;136(Pt 1):181-95.
36. Marin-Padilla M. Mesodermal alterations induced by hypervitaminosis A. J Embryol Exp Morphol 1966;15:261-9.
37. Marin-Padilla M, Marin-Padilla TM. Morphogenesis of experimentally induced Arnold--Chiari malformation. J Neu-

 https://doi.org/10.14245/ns.2551050.525

rol Sci 1981;50:29-55.
38. Marín-Padilla M. Cephalic axial skeletal-neural dysraphic disorders: embryology and pathology. Can J Neurol Sci 1991; 18:153-69.
39. Nakanishi N, Sakamoto H, Nishikawa M, et al. Pathogenesis of encephaloschisis in retinoic-acid-treated hamster embryos I: a morphometric study of the craniofacial structures. J Craniofac Genet Dev Biol 1999;19:174-82.
40. Capra V, Iacomino M, Accogli A, et al. Chiari malformation type I: what information from the genetics? Childs Nerv Syst 2019;35:1665-71.
41. Markunas CA, Enterline DS, Dunlap K, et al. Genetic evaluation and application of posterior cranial fossa traits as endophenotypes for Chiari type I malformation. Ann Hum Genet 2014;78:1-12.
42. Miró X, Zhou X, Boretius S, et al. Haploinsufficiency of the murine polycomb gene Suz12 results in diverse malformations of the brain and neural tube. Dis Model Mech 2009;2: 412-8.
43. Urbizu A, Khan TN, Ashley-Koch AE. Genetic dissection of Chiari malformation type 1 using endophenotypes and stratification. J Rare Dis Res Treat 2017;2:35-42.
44. Urbizu A, Garrett ME, Soldano K, et al. Rare functional genetic variants in COL7A1, COL6A5, COL1A2 and COL5A2 frequently occur in Chiari malformation type 1. PLoS One 2021;16:e0251289.
45. Fries FN, Hendrix P, Brinker TJ, et al. Otto Mennicke (1876-) and the first description of skull base anomalies causing cerebellar tonsillar ectopia: one of the first mentions of the Chiari I malformation. Childs Nerv Syst 2017;33:825-7.
46. Knight J, De Jesus O. Tonsillar Herniation. 2023 Aug 23. In: StatPearls [Internet]. Treasure Island (FL): StatPearls Publishing; 2025 Jan–.
47. Srour M, Caron V, Pearson T, et al. Gain-of-function mutations in RARB cause intellectual disability with progressive motor impairment. Hum Mutat 2016;37:786-93.
48. Maden M. Retinoic acid in the development, regeneration and maintenance of the nervous system. Nat Rev Neurosci 2007;8:755-65.
49. Niederreither K, Dollé P. Retinoic acid in development: towards an integrated view. Nat Rev Genet 2008;9:541-53.
50. Di Rocco F, Biosse Duplan M, Heuzé Y, et al. FGFR3 mutation causes abnormal membranous ossification in achondroplasia. Hum Mol Genet 2014;23:2914-25.
51. Twigg SR, Vorgia E, McGowan SJ, et al. Reduced dosage of ERF causes complex craniosynostosis in humans and mice and links ERK1/2 signaling to regulation of osteogenesis. Nat Genet 2013;45:308-13.
52. Kawachi K, Masuyama N, Nishida E. Essential role of the transcription factor Ets-2 in Xenopus early development. J Biol Chem 2003;278:5473-7.
53. Brockmeyer DL, Cheshier SH, Stevens J, et al. A likely HOXC4 predisposition variant for Chiari malformations. J Neurosurg 2022;139:266-74.
54. Abbott D, Brockmeyer D, Neklason DW, et al. Population-based description of familial clustering of Chiari malformation type I. J Neurosurg 2018;128:460-5.
55. Matsuoka T, Ahlberg PE, Kessaris N, et al. Neural crest origins of the neck and shoulder. Nature 2005;436:347-55.
56. Poretti A, Mall V, Smitka M, et al. Macrocerebellum: significance and pathogenic considerations. Cerebellum 2012;11: 1026-36.
57. Raybaud C, Jallo GI. Chiari 1 deformity in children: etiopathogenesis and radiologic diagnosis. Handb Clin Neurol 2018; 155:25-48.
58. Conway RL, Danielpour M, Graham JM Jr. Surgical management of cerebellar tonsillar herniation in three patients with macrocephaly-cutis marmorata telangiectatica congenita. Report of three cases. J Neurosurg 2007;106(4 Suppl):296-301.
59. Milhorat TH, Bolognese PA, Nishikawa M, et al. Association of Chiari malformation type I and tethered cord syndrome: preliminary results of sectioning filum terminale. Surg Neurol 2009;72:20-35.
60. Nishikawa M, Milhorat TH, Bolognese PA, et al. Tethered cord syndrome: preliminary report of clinical features and morphometric analyses on association of Chiari malformation type I. Spinal Surg 2009;23:195-203.
61. McLone DG, Knepper PA. The cause of Chiari II malformation: a unified theory. Pediatr Neurosci 1989;15:1-12.
62. Milhorat TH, Bolognese PA, Nishikawa M, et al. Syndrome of occipitoatlantoaxial hypermobility, cranial settling, and chiari malformation type I in patients with hereditary disorders of connective tissue. J Neurosurg Spine 2007;7:601-9.
63. Nishikawa M, Milhorat TH, Bolognese PA, et al. Occipito-atlanto-axial hypermobility: clinical features and dynamic analyses of cranial settling and posterior gliding of occipital condyle. Spinal Surg 2009;23:168-75.
64. Boyles AL, Enterline DS, Hammock PH, et al. Phenotypic definition of Chiari type I malformation coupled with high-density SNP genome screen shows significant evidence for linkage to regions on chromosomes 9 and 15. Am J Med

Genet A 2006;140:2776-85.
65. Sadler B, Wilborn J, Antunes L, et al. Rare and de novo coding variants in chromodomain genes in Chiari I malformation. Am J Hum Genet 2021;108:100-14.
66. Provenzano A, La Barbera A, Scagnet M, et al. Chiari 1 malformation and exome sequencing in 51 trios: the emerging role of rare missense variants in chromatin-remodeling genes. Hum Genet 2021;140:625-47.
67. Ellington M, Francomano CA. Chiari I malformations and the heritable disorders of connective tissue. Neurosurg Clin N Am 2023;34:61-5.
68. Oaks J. Chiari malformation and syringomyelia. In: Regachary SS, Williams RH, editors. Principles of neurosurgery. London: Mosby-Wolf; 1994. p. 9.1.189.
69. Sakamoto H, Nishikawa M, Hakuba A, et al. Expansive suboccipital cranioplasty for the treatment of syringomyelia associated with Chiari malformation. Acta Neurochir (Wien) 1999;141:949-60; discussion 960-1.
70. Winegar CD, Lawrence JP, Friel BC, et al. A systematic review of occipital cervical fusion: techniques and outcomes. J Neurosurg Spine 2010;13:5-16.
71. Milhorat TH, Bolognese PA. Tailored operative technique for Chiari type I malformation using intraoperative color Doppler ultrasonography. Neurosurgery 2003;53:899-905; discussion 905-6.
72. Nishikawa M, Ohata K, Baba M, et al. Chiari I malformation associated with ventral compression and instability: one-stage posterior decompression and fusion with a new instrumentation technique. Neurosurgery 2004;54:1430-4; discussion 1434-5.
73. Oldfield EH, Muraszko K, Shawker TH, et al. Pathophysiology of syringomyelia associated with Chiari I malformation of the cerebellar tonsils. Implications for diagnosis and treatment. J Neurosurg 1994;80:3-15.
74. Heiss JD, Patronas N, DeVroom HL, et al. Elucidating the pathophysiology of syringomyelia. J Neurosurg 1999;91:553-62.
75. Hirabayashi K. Japanese orthopaedic association score in cervical spondylotic myelopathy. Nippon Seikeigekagakkai Zassi 1994;68:490-503. Japanese.
76. Holly LT, Batzdorf U. Chiari malformation and syringomyelia. J Neurosurg Spine 2019;31:619-28.
77. Klekamp J. Surgical treatment of Chiari I malformation--analysis of intraoperative findings, complications, and outcome for 371 foramen magnum decompressions. Neurosurgery 2012;71:365-80; discussion 380.
78. Luciano MG, Batzdorf U, Kula RW, et al. Development of common data elements for use in Chiari malformation type i clinical research: an NIH/NINDS project. Neurosurgery 2019;85:854-60.
79. McClugage SG, Oakes WJ. The Chiari I malformation. J Neurosurg Pediatr 2019;24:217-26.
80. Nishikawa M, Bolognese PA, Kula RW, et al. Surgical management of Chiari malformations: preliminary results of surgery according to the mechanisms of ptosis of the brain stem and cerebellum. J Neurol Surg B Skull Base 2021;82:264-72.
81. Nishikawa M, Bolognese PA, Yamagata T, et al. Surgical management of Chiari malformation type I and instability of the craniocervical junction based on its pathogenesis and classification. Neurol Med Chir (Tokyo) 2022;62:400-15.
82. Nishikawa M, Yamagata T, Naito K, et al. Surgical management of Chiari malformation type i associated with syringomyelia: outcome of surgeries based on the new classification and study of cerebrospinal fluid dynamics. J Clin Med 2022;11:4556.
83. Goel A, Bhatjiwale M, Desai K. Basilar invagination: a study based on 190 surgically treated patients. J Neurosurg 1998;88:962-8.
84. Menezes AH. Craniocervical developmental anatomy and its implications. Childs Nerv Syst 2008;24:1109-22.

 https://doi.org/10.14245/ns.2551050.525